1	An investigation of Rhinovirus Infection on Cellular Uptake of Poly (glycerol-adipate)
2	Nanoparticles
3	
4	Yasmin Abo-zeid ^{1,2,3} , Gareth R. Williams ² , Lila Touabi ³ , Gary R. McLean ^{3,4}
5	
6	¹ Faculty of Pharmacy, Helwan University, Cairo, Egypt
7	² UCL School of Pharmacy, University College London, 29 – 39 Brunswick Square, London
8	WC1N 1AX, UK
9	³ Cellular and Molecular Immunology Research Centre, London Metropolitan University, 166-
10	220 Holloway Road, London, N7 8DB, UK
11	⁴ National Heart and Lung Institute, Imperial College London, Norfolk Place, London W2 1PG
12	UK
13	Corresponding Author:
14	Yasmin Abo-zeid ^{1, 2, 3}
15	E-mail: yasmin.abozeid@pharm.helwan.edu.eg
16	Mobile : +201092892746
17	
18	Co-Authors:
19	Gareth R. Williams ²
20	E-mail: g.williams@ucl.ac.uk
21	Lila Touabi ³
22	E-mail: <u>lit0208@my.londonmet.ac.uk</u>
23	

24	Gary	R.	McI	Lean ^{3,4}

E-mail: <u>g.mclean@londonmet.ac.uk</u>

28 Abstract:

Viral infections represent 44% of newly emerging infections, and as is shown by the COVID-19 29 30 outbreak constitute a major risk to human health and wellbeing. Although there are many efficient antiviral agents, they still have drawbacks such as development of virus resistance and 31 32 accumulation within off-target organs. Encapsulation of antiviral agents into nanoparticles (NPs) has been shown to improve bioavailability, control release, and reduce side effects. However, there 33 is little quantitative understanding of how the uptake of NPs into virally infected cells compares 34 35 to uninfected cells. In this work, the uptake of fluorescently labeled polymer NPs was investigated in several models of rhinovirus (RV) infected cells. Different multiplicities of RV infections (MOI) 36 and timings of NPs uptake were also investigated. In some cases, RV infection resulted in a 37 significant increase of NPs uptake, but this was not universally noted. For HeLa cells, RV-A16 38 and RV-A01 infection elevated NPs uptake upon increasing the incubation time, whereas at later 39 40 timepoints (6h) a reduced uptake was noted with RV-A01 infection (owing to decreased cell viability). Beas-2B cells exhibited more complex trends: decreases in NPs uptake (cf. uninfected 41 cells) were observed at short incubation times following RV-A01 and RV-A16 infection. At later 42 43 incubation times (4h), we found a marked decrease of NPs uptake for RV-A01 infected cells but an increase in uptake with RV-A16 infected cells. Where increases in NPs uptake were found, they 44 45 were very modest compared to results previously reported for a hepatitis C/Huh7.5 cell line model. An increase in RV dose (MOI) was not associated with any notable change of NPs uptake. We 46 argue that the diverse endocytic pathways among the different cell lines, together with changes in 47 48 virus nature, size, and entry mechanism are responsible for these differences. These findings suggest that NPs entry into virally infected cells is a complex process, and further work is required 49

50	to unravel the different factors which govern this. Undertaking this additional research will be
51	crucial to develop potent nanomedicines for the delivery of antiviral agents.
52	
53	Keywords: Polymer nanoparticles; Poly (glycerol-adipate); virus infection; nanoparticle uptake;

54 HeLa and Beas-2B cells

59 Viral infections represent a public health problem with a major negative impact on health, 60 socioeconomic development and are the biggest pandemic threat in the modern era (Adalja and Inglesby, 2019; Nii-Trebi, 2017). This is clearly evidenced by the 2020 COVID-19 pandemic. All 61 62 the top priority emerging infectious diseases with the greatest risk of epidemic or pandemic potential are viral diseases (Nii-Trebi, 2017). There are more than 90 antiviral agents in the market 63 64 (Clercq and E., 2016), but most of them are highly specific to one virus or to members of a viral 65 family and are inactive against other viruses (Adalja and Inglesby, 2019). The high rate of virus 66 mutation, development of antiviral resistance (Irwin et al., 2016), and preponderance of side effects with long term administration of antiviral agents (Chawla et al., 2018) are additional challenges. 67 For example, mitochondrial toxicity recorded with nucleoside reverse transcriptase inhibitors 68 could be lethal (Moyle, 2000). The emergence of new viruses such as SARS-CoV-2 (Pradhan et 69 70 al., 2020; Zhang et al., 2020) leads to high morbidity rates (Abo-Zeid et al., 2020; Nii-Trebi, 2017; Peters and LeDuc, 1999; Pradhan et al., 2020; Shanks and Brundage, 2012; Zhang et al., 2020) 71 since existing antivirals are often not effective. These challenges require the discovery of new 72 73 approaches to control virus infections. Broad spectrum antiviral agents are one option; however, there are few of them available for clinical application, and their administration is associated with 74 75 side effects due to accumulation at off-target organs (such as that observed with ribavirin) (Oventa 76 et al., 2000; Soota and Maliakkal, 2014).

77

Nanomedicine could be considered as an alternative strategy to improve the treatment of viral infections. In the scientific literature (Lembo et al., 2018), encapsulation of antiviral agents into nanoparticles (NPs) was found to overcome several limitations of conventional antiviral agents

(Szunerits et al., 2015), such as short half-lives and high frequency of drug administration (Harvie 81 et al., 1996) and instability in vivo (Ochekpe et al., 2009). NPs can also improve the delivery of 82 hydrophilic drug into cells (Hillaireau et al., 2006), overcome side effects (Moyle, 2000), improve 83 bioavailability of poorly soluble antiviral agents (Gaur et al., 2014), control/sustain drug release 84 (Lembo et al., 2013), and aid crossing the blood brain barrier (Fiandra et al., 2015); (Nowacek, 85 2010). However, the effect of virus infection on the uptake of NPs has not been studied in detail. 86 To the best of our knowledge, until very recently no studies attempted to quantify NPs uptake by 87 88 virus infected cells in comparison to un-infected cells. The effect of viral infection on NPs uptake is however an important consideration. NPs are mainly taken up into cells by an endocytic pathway 89 90 (Foroozandeh and Aziz, 2018) and possibly a down-regulation of endocytosis because of viral 91 infection would make NPs delivery of the appropriate antiviral agent(s) less effective.

92

We previously (Abo-zeid et al., 2018b) tracked the uptake of poly(glycerol-adipate) nanoparticles 93 94 fluorescently labelled with rhodamine B isothiocyanate (RBITC PGA NPs) in human hepatoma cells (Huh7.5 cells) transfected with the hepatitis C virus (HCV) J6/JFH1 chimera (a recombinant 95 HCV designed for maximum replication and virion production in vitro). Confocal microscopy 96 demonstrated an enhancement of NPs uptake by infected cells in comparison to non-transfected 97 cells, and by performing flow cytometric analyses, we found that virus transfected cells showed 98 significantly (> 2 times) increased NPs uptake over non-transfected cells. The NPs were not 99 decorated with any ligands to target specific receptors at the surface of Huh7.5 cells. Therefore, a 100 change in cellular physiology due to viral infection was hypothesized to be the driving force 101 responsible for the enhanced NPs uptake. 102

104	In this study, we have investigated if this concept could be further extended to other viruses. We
105	tracked the uptake of RBITC PGA NPs into four models of virus infected cells: (1) HeLa cervical
106	cancer cells infected with rhinovirus A16 (RV-A16), (2) HeLa cells infected with rhinovirus A01
107	(RV-A01), (3) Beas-2B bronchial epithelial cells infected with RV-A16 and (4) Beas-2B cells
108	infected with RV-A01. Non-infected HeLa and Beas-2B cells were employed as controls. These
109	cell lines were chosen because they have diverse biological characteristics and can be infected with
110	RVs. HeLa is a human cervical carcinoma cell line routinely used for the propagation of RVs
111	(Arruda et al., 1997). Beas-2B is a human bronchial epithelial cell line transformed in vitro to grow
112	continuously (Reddel et al., 1988) by infection with $SV40$ or adenovirus-12 $SV40$ hybrid virus .
113	Both HeLa and Beas-2B cell lines can be infected with RVs (Bartlett et al., 2012) as they express
114	the major group RV receptor ICAM-1 (Greve et al., 1989) and the minor group RV entry receptor
115	LDLR (Hofer et al., 1994).
116	
117	RVs infect the airway epithelium, are considered the most frequent cause of the common cold
118	(Mäkelä et al., 1998). They are also associated with acute exacerbations of asthma and COPD
119	(Johnston et al., 1995; Nicholson et al., 1993; Papi et al., 2006). RVs have further been implicated
120	in acute otitis media, sinusitis, and lower respiratory tract disease (Henquell et al., 2012; Kiang et

al., 2007; Winther, 2011). In the current work, RV-A16 and RV-A01 were used as the viruses for
study because they are not highly pathogenic (level II pathogens) and represent both the major and
minor groups of RVs respectively, entering cells via different entry receptors and endocytic
uncoating mechanisms (Schuler et al., 2014). Although both major and minor group RVs enter the
endocytic pathway of cells (Fuchs and Blaas, 2009), they are thought to leave endosomes by
different mechanisms (Schober et al., 1998). Thus, the use of diverse cells, viruses, entry and

uncoating mechanisms should enable us to elucidate if the enhanced uptake of NPs previously
reported (Abo-zeid et al., 2018b) with hepatitis C infected Huh7.5 cells is a general phenomenon
applicable to all virus infected cells, or whether cell and infection type has an effect on the NPs
uptake process.

131

132 **2-** Materials and methodology:

133

134 **2.1. Materials:**

Rhinovirus stocks, HeLa and Beas-2b cells were provided by Prof S Johnston, National Heart and
Lung Institute, Imperial College London. DMEM medium, RPMI medium, fetal calf serum (FCS),
non-essential amino acids (NEAA), anti-human ICAM-1-FITC, penicillin, and streptomycin were
supplied by Thermo Fisher. All other materials were purchased from Sigma-Aldrich and used as
supplied.

140

141 **2.2. Methodology:**

142 2.2.1. Synthesis and characterization of poly(glycerol-adipate):

The polymer was synthesized following a literature protocol (Abo-zeid et al., 2018a). Briefly, poly(glycerol-adipate) (PGA) was synthesized by dissolving equal amounts (250 mmol) of glycerol and divinyl-adipate (DVA) in dry tetrahydrofuran (THF, 30 ml) in presence of a catalytic enzyme, novozyme 435 (1.25g). The reaction mixture was stirred (overhead stirrer, 200 rpm) at constant temp (50°C) for 24 h. This was followed by enzyme filtration and evaporation of THF to obtain a yellowish jelly-like polymer. This polymer was characterized by gel permeation chromatography (GPC) and ¹H-NMR.

150 GPC were performed following our previous protocol (Abo-zeid et al., 2018a; Kallinteri et al., 2005) using a Polymer Laboratories system, employing 2 mixed bed (D) columns at 40 °C, flow 151 rate 1 ml/min in THF, using an evaporative light scattering detector which was calibrated with 10 152 narrow polystyrene standards. MALDI-TOF data was collected on an Applied Biosystems QSTAR 153 (Q-ToF) mass spectrometer for determination of polymer molecular weight and molecular weight 154 dispersity (D). Briefly, polymer samples (20 mg) were dissolved in THF (2 ml) and the solutions 155 were mixed for an hour on a roller-mixer (SRT1, Stuart) to allow the polymer to fully dissolve. 156 157 This was followed by sample filtration using a syringe membrane nylon filter (0.2 μ m) before the same was analyzed by size exclusion chromatography and mass spectrometer. ¹H-NMR spectra 158 159 were recorded on Bruker AVIII HD 400 MHz NMR using a BBFO+ probe and are expressed in 160 parts per million (δ) from internal tetramethylsilane. Polymer and DVA samples were dissolved in acetone-d₆ while glycerol was dissolved in DMSO-d₆ as previously reported (Abo-zeid et al., 161 2018a). 162

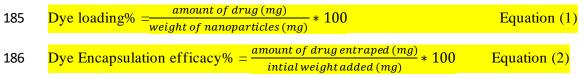
163

164 2.2.2. Preparation and characterization of RBITC PGA NPs:

RBITC PGA NPs were prepared and fluorescent dye loading was optimized as previously reported 165 (Abo-zeid et al., 2018b; Abo-zeid and Garnett, 2020). Briefly, RBITC (200 µl, 1 mg/ml, in 166 methanol) was added into an aqueous phase (HEPES buffer, 10 mM, pH 7.4, 7 ml). The polymer 167 (20 mg) was dissolved in acetone (2 ml) and then added dropwise into the aqueous phase under 168 169 stirring. The sample was left to stir overnight for complete removal of the organic solvent. RBITC PGA NPs were purified by loading the sample onto a Sephacryl S-200-HR gel column (C2.5 X 170 171 40, Pharmacia, bed volume 91 ml). The column was eluted by water using an AKTA prime plus liquid chromatography system (GE Healthcare Life Sciences) at a flow rate of 1 ml/min and 172

173	collected in fractions of 1.5 ml per tube. The peaks of dye labelled NPs and free dye were detected
174	using a UV detector at 214 nm. The purified NPs dispersion was collected for particle size and
175	zeta potential analysis. Samples were diluted in HEPES buffer (1mM, pH 7.4) to give a count rate
176	ranged between 50 to 300 Kcps and measurements were performed at 25 $^\circ\text{C}\pm0.1$ using Malvern
177	Zeta sizer Nano ZS (Malvern Instruments Ltd, Malvern, UK). The dye loading and encapsulation
178	percentages were determined by a direct method, a weighed amount of freeze dried RBITC PGA
179	NPs was extracted in acetone: methanol (1:1 v/v). The fluorescence was measured at $\lambda_{Ex} = 545$ nm
180	and $\lambda_{Em} = 575$ nm using a Hitachi F-4500 spectrophotofluorometer with slit widths adjusted to 5
181	nm. The concentration of RBITC was quantified using a pre-determined calibration curve prepared
182	in the same solvent system. Dye loading and dye encapsulation percentages were calculated using
183	Equations 1 and 2 respectively.
184	

184



187

188 2.2.3. RVs propagation and tissue culture infectious dose 50% (TCID50) determination:

HeLa cells were grown in T175 flasks in DMEM containing, FCS (10% v/v), penicillin and streptomycin solution (1% v/v). After reaching 80% confluence, cells were used to propagate the virus. The previous medium was removed, and cells were infected with RVs in the presence of DMEM and FCS (2% v/v), penicillin and streptomycin solution (1% v/v). To enhance virus attachment, the flask was gently shaken for 1 h at room temperature. Cultures were incubated for 24 h at 37 °C and 5% CO₂ where a cytopathic effect (CPE) greater than 80% was achieved. Cells were then subjected to three freeze-thawing cycles and vortexed briefly to lyse cells and release 196 cell-associated virus. Virus was clarified by centrifugation (4000 rpm, 15 min). Supernatant 197 containing virus was collected, aliquoted and stored at -80° C.

198

199 RV stock solution was titred by infecting a HeLa cell monolayer $(1.5 \times 10^4 / \text{well})$ in a 96 well 200 microtiter plate using a serial diluted virus $(10^{-1} \text{ to } 10^{-9})$ in DMEM in presence of FCS (4% v/v), 201 penicillin and streptomycin solution (1% v/v). Plates were incubated at 37 °C and 5% CO₂ for 3 202 to 4 days and then wells were scored for presence or absence of CPE by microscopic examination 203 to determine TCID50. The TCID50 refers to the final dilution of RV where there is evidence of 204 infection of 50% of the cultured wells.

205

206 **2.2.4. Cell viability after RV infection:**

207

HeLa or Beas-2B cells $(4 \times 10^4 / \text{well})$ were seeded into 24-wells plate. Culture medium [1 ml; either 208 DMEM or RPMI with FCS (10% v/v) and penicillin and streptomycin solution (1% v/v)] was 209 added respectively to HeLa and Beas-2B cells followed by incubation for 24 h at 37 °C and 5% 210 CO₂. Thereafter, the culture media were removed, and cells were treated with virus solutions (1 211 212 ml) of different multiplicity of infection (MOI): 0.03, 0.3, 0.5, 0.7 and 1. The virus solution comprised RV suspended in DMEM or RPMI in presence of FCS (2% v/v), penicillin and 213 streptomycin solution (1%, v/v). Cells were gently shaken with virus solution for 1 h at room 214 215 temperature to allow attachment, followed by removal of virus solution and addition of fresh culture medium [1 ml; DMEM or RPMI with FCS (2% v/v) and penicillin/streptomycin solution 216 (1%, v/v)] to the HeLa and Beas-2B cells respectively. Cells were incubated at 37 °C and 5% CO₂ 217 for 24 h. This was followed by removal of culture medium from all cells and addition of Alamar 218 219 Blue (AB) solution (1 ml, 36 µg/ml) into each well followed by incubation in the dark at 37 °C and 5% CO₂ for 6 h to determine the cells viability. AB solution (36 μ g/ml) was prepared by dissolving AB in DMEM or RPMI containing FCS (2% v/v) and penicillin/streptomycin solution (1% v/v) for HeLa cells and Beas2B cells respectively. The fluorescence was measured at excitation and emission wavelengths of 540 and 595 nm respectively using a FLUOstar Omega multi-mode microplate reader (BMG Labtech). Negative (AB solution without cells) and positive (AB solution autoclaved for 15 min) controls were also included in the plate. Two independent experiments were performed where each sample was prepared in triplicate.

227

228 2.2.5. RV PCR to determine infection:

HeLa cells infected with RV-A16 at MOI 0.5 were placed in a humidified 37 °C incubator at 5% 229 CO₂ and were lysed with RLT buffer (Qiagen) after 2, 4, 8, 24 and 48 h of incubation. RNA was 230 extracted from cells using the RNeasy Mini Kit (Qiagen) following the manufacturer's protocol. 231 Purified RNA samples were reverse transcribed using a RevertAid reverse transcriptase and first 232 strand cDNA synthesis kit (Fisher Scientific) following the manufacturer's instructions. For 233 random hexamer primed synthesis, the reaction mix was incubated for 5 min at 25 °C followed by 234 60 min at 42 °C, and for Oligo (Dt)18 the synthesis reaction mix was incubated for 60 min at 42 235 ${}^{0}C.$ 236

1µl of cDNA was added to a reaction mix of 49 µl containing PCR buffer, forward and reverse
primers (RV-A16 primers were: forward: TATAAAGCTTTCCAAAGGTTGGTCGTG; reverse:
TATACTCGAGCTAAGCTAACTGGTGTTC3'), deoxynucleotide triphosphates dNTPs and Taq
polymerase (Fisher Scientific). After an initial denaturing step of 95 °C for 3 min, PCR was run
for 40 cycles of 95 °C for 30 s, 52 °C for 30 s, 72 °C for 1 min and a final extension of 72 °C for 5
min. Similar conditions were used for amplification of the control gene glyceraldehyde-3-

243 phossphate dehydrogenase (gapdh) using forward and reverse primers244 GTCTCCTCTGACTTCAA and ACCACCCTGTTGCTGTA.

245

246 **2.2.6.** NPs uptake by cells:

HeLa or Beas-2B cells were seeded into 6-well plates (1.15 x 10^{5} /well), followed by addition of 247 comprising DMEM or RPMI with FCS (10% v/v) culture medium (2ml) 248 and 249 penicillin/streptomycin solution (1% v/v) respectively. The cells were incubated at 37 $^{\circ}$ C and 5% 250 CO₂ for 24 h. Culture media were removed, and cells were infected with RV at MOI of 0.5 for HeLa cells and MOI of both 0.5 and 1 in the case of Beas-2B cells. Cells were gently shaken with 251 252 RV for 1 h at room temperature to allow attachment, followed by removal of virus solution and 253 addition of fresh culture medium (2 ml) containing FCS (2% v/v) before the cells were incubated 254 at 37 °C and 5% CO₂ for 24 h. Culture medium was removed and a RBITC PGA NPs colloidal suspension (1.8 ml, 510 µg NPs) added into each well. The colloidal suspension was prepared by 255 256 adding a purified NPs suspension (850 µl, 510 µg) into an equal volume of FCS, followed by 257 incubation for 24 h. The isotonicity of the NPs suspension was adjusted with phosphate buffered saline (one tablet of PBS was dissolved in 10 ml instead of 100ml to yield 10 times concentrated 258 PBS solution) prior to addition to cells. Cells were incubated for different time intervals. Next, the 259 suspension was removed, and cells were washed with PBS (2 ml, 3 washes). Cell dissociation 260 buffer enzyme-free PBS (0.5 ml) was added to each well and the plate incubated for 10 min to 261 262 detach cells. The cells were collected and centrifuged (4000 rpm, 15 min). The supernatant was removed, and cells were washed with PBS (2 ml, 3 washes). Cells were then fixed with 263 264 paraformaldehyde in PBS (1 ml, 2% v/v). A set of non-infected cells were treated similarly but without addition of RV. NPs uptake was tracked using flow cytometry (Guava easyCyte 8HT, 265

MerckMillipore). The settings of the instrument were adjusted as follows: (1) blank cells (HeLa or Beas-2B cells that were not treated with NPs or virus solution) were used to create scatter plots to observe events; (2) non-infected cells (HeLa or Beas-2B cells) previously incubated with RBITC PGA NPs for 6 h were observed by adjusting the setting of the yellow fluorescence channel. Some cells were also stained with anti-human ICAM-1-FITC by incubating on ice for 20 min with diluted antibodies followed by PBS washing and fixing with paraformaldehyde in PBS (2% v/v).

273

274 **2.2.7. Statistical analysis:**

All statistical analysis was performed using two-way ANOVA followed by a post-hoc Tukey test.
Analyses were carried out by GraphPad Prism 8.0 software at confidence level (95%, 99% and 99.9%).

278 **3. Results:**

279 **3.1. Synthesis of PGA:**

The successful synthesis of PGA was confirmed by ¹H NMR (Figure S1 and S2, Supplementary Information), with the data agreeing with the literature (Abo-zeid et al., 2018a). Size exclusion chromatography analysis gave an estimated Mn of 11.6 kDa, molecular weight dispersity Đ of 1.4, and molecular weight (Mw) of 16 kDa.

284

285 **3.2. Preparation of nanoparticles:**

RBITC PGA NPs were prepared by interfacial deposition and fluorescent dye loading was achieved as previously reported (Abo-zeid et al., 2018b; Abo-zeid and Garnett, 2020). The particle size was 110 ± 30 nm (diameter mean \pm SD) and the polydispersity index 0.01, indicating a monodisperse sample. The zeta potential was -53.7 ± 13.3 mv indicating a stable dispersion. The encapsulation efficiency and dye loading were 54 ± 13 % and 0.54 ± 0.13 %, respectively. This dye loading is sufficient enough to track NPs uptake by cells using flow cytometry (Abo-zeid et al., 2018b; Abo-zeid and Garnett, 2020).

293

3.3. Virus infection of cells:

295 Infection of HeLa cells is used routinely for RV propagation (Arruda et al., 1996) and infection of 296 the human bronchial cell line Beas-2B by RV-A16 and RV-A01 has been shown previously (Bartlett et al., 2012). We made new RV preparations for these studies and demonstrated the 297 TCID50/ml to be 2.96x10⁷ for RV-A16 and 3.9 x 10⁷ for RV-A01. To establish conditions of RV 298 299 infection resulting in minimal cytotoxicity of HeLa and Beas-2B cells and allowing the 300 investigation of NPs uptake into cells, varying multiplicity of infection (MOI) of both RV-A01 and RV-A16 was also tested. We found that an increase of MOI was associated with a decrease of 301 302 cell viability in both HeLa and Beas-2B cells infected with both viruses (Table 1). The viability of 303 HeLa cells was reduced compared to that of Beas-2B cells at higher MOI, and RV-A01 resulted in more cytotoxic effects than RV-A16 in HeLa cells. Only minor effects on the viability of Beas-304 2B cells were observed with both RV serotypes. For subsequent experiments with NPs, an RV 305 MOI of 0.5 was chosen for HeLa cells and MOI of both 0.5 and 1.0 for Beas-2B cells. 306

- 307
- 308
- 309

Table 1: Percentage viability of HeLa and Beas-2B cells after RV infection at indicated MOI. Data are shown as mean (standard deviation). Results are average of two independent experiments with three replicates in each

RV-A01 100 (6)	RV-A16 106 (5)	RV- A01 108 (7)
100 (6)	106 (5)	108 (7)
		100 (7)
94 (5)	106 (8)	105 (8)
80 (5)	101 (11)	98 (10)
73 (8)	101 (6)	99 (9)
	102 (5)	97 (6)
	66 (5)	66 (5) 102 (5)

³¹⁰

To prove RV infection of cells in the absence of sustained cytopathic effects, we performed PCR to detect the RV genome. Using HeLa cells infected with RV-A16 at MOI of 0.5, RT-PCR was performed on RNA samples obtained from uninfected and RV-infected cells at several timepoints (Figure 1). RV-A16 genome was detected in HeLa cells 24 and 48 h after initiation of infection but not at earlier timepoints. Since the same RV preparations were used to infect Beas-2B cells it was assumed that MOI of 0.5 and 1 will be sufficient to cause infection, as has been shown previously (Bartlett et al., 2012).

318

319 **3.4. Nanoparticle uptake by cells:**

Having established infection conditions that resulted in infected cells but minimal cytopathic effects, we next studied the effect of RV infection on the uptake of NPs into cells. We also investigated expression levels of the RV major group entry receptor intercellular adhesion molecule-1 (ICAM-1) on infected cells. Figure 2A demonstrates that HeLa cells express ICAM- 1, and that expression levels are not altered by RV infection. Incubation with NPs for 6 h resulted
in complete uptake of NPs into HeLa cells (lower right quadrant, Figure 2A) that were shown to
be ICAM-1 positive (upper right quadrant, Figure 2B). No significant differences in NPs uptake
were observed between uninfected and RV-A16 infected cells after incubation with NPs for 6 h
(Figure 2B). However, a reduction in NPs uptake by RV-A01 infected cells was noted (Figure 2B).
This reduced uptake is most likely due to the lower viability of these infected cells as shown in
Table 1.

331

Flow cytometry contour plots for the time course analysis of NPs uptake in the absence of ICAM-332 1 staining are given (Figure 3). The lower left (LL) quadrant represents cells with a low 333 334 fluorescence signal for RBITC at baseline and shifts to the lower right (LR) quadrant reflect an increase of RBITC fluorescence intensity indicative of NPs uptake. All cells, either infected or 335 non-infected, showed a shift from the LL to LR quadrant with increased incubation times. These 336 337 data are shown both as percentages of gated cells within the contour plots and as a quantitative number of cells, revealing that similar numbers of events have been analyzed within each condition 338 (Figure 3). The cell numbers appear slightly different because virus infection affects the cells 339 viability, as was discussed earlier in Section 3.3. 340

341

The percentage of positive cells for both uninfected and infected cells increases with the time of incubation with RBITC PGA NPs (Figure 4A), but there is a small reduction within infected cells. Quantitative flow cytometry analysis of NPs uptake in uninfected and infected HeLa cells is presented (Figure 4B) as mean fluorescent intensity (MFI), from which it is apparent that uninfected cells display a comparable MFI to RV-A16 infected cells at 0, 2 and 4h but there is a significant (P < 0.05) increase of MFI for RV-A16 cells at 6 h. RV-A01 infected cells demonstrated a significantly (P < 0.01) higher MFI than uninfected cells at all timepoints except 6 h, where the MFI was significantly (P < 0.001) lower. The latter is matched with the lower percentage of positive cells recorded at 6 h for RV-A01 infected cells.

351

Flow cytometry histograms demonstrating the uptake of NPs with time in uninfected and infected 352 353 Beas-2B cells are depicted in Figure 5A. Both uninfected and infected cells demonstrated an 354 increase in RBITC fluorescence over control cells (cells that were not incubated with NPs, grey filled) at 1 h (red line) and 4 h (blue line) at MOI of both 0.5 and 1. Quantitative flow cytometry 355 356 plots (Figure 5B) show a similar trend of NPs uptake at MOI of 0.5 and 1. Here, uninfected cells 357 showed a significantly (P < 0.01) higher uptake of NPs than infected cells after incubation for 1 h, but upon increasing the incubation time to 4 h RV-A16 infected cells showed significantly higher 358 NPs uptake than uninfected cells (P < 0.001 and P < 0.01 at MOI of 0.5 and 1 respectively). The 359 360 opposite was observed with RV-A01 infection, where NPs uptake was significantly lower than uninfected cells (P < 0.001 and P < 0.01 at MOI of 0.5 and 1). 361

362

363 **4. Discussion:**

Infectious diseases include those caused by bacteria, parasites, fungi and viruses. Virus infections are considered the most challenging due to high rates of virus mutation resulting in new strains that can escape immunity and/or are resistant to antiviral agents, and adverse side effects associated with prolonged administration of antiviral agents. All of these result in reduction in the effectiveness of antiviral therapies. Encapsulation of antiviral agents into NPs has previously been reported to overcome the drawbacks of conventional therapy (Lembo et al., 2018). However, when looking at the literature we could not identify studies investigating the effect of virus infection on

371	the quantitative uptake of NPs. We reported in 2018 (Abo-zeid et al., 2018b) a significant two fold
372	increase of NPs uptake in a HCV-infected liver cell line over that recorded with uninfected cells.
373	

This study explored four different models of virally infected cells to broaden our understanding 374 into the effect of infection on NPs uptake. We prepared fluorescently labelled RBITC PGA NPs 375 with a dye loading that is sufficient to track the uptake of NPs by flow cytometry (Abo-zeid et al., 376 377 2018b; Abo-zeid and Garnett, 2020). These NPs were used for several reasons: they are formulated 378 from PGA, a biodegradable and biocompatible polymer with very low cytotoxic properties (Abozeid and Garnett, 2020; Zhang et al., 2014; Kallinteri et al., 2005;), and RBITC is retained in the 379 380 NPs for a prolonged period of time (Meng et al., 2006), allowing us to track the uptake of NPs 381 rather than free dye (Abo-zeid et al., 2018b). RBITC dye gives a good fluorescence in the acidic pH of lysosomal compartment (Garnett and Baldwin, 1986) leading to effective detection of NPs 382 taken up by cells using flow cytometry (Abo-zeid and Garnett, 2020; Abo-zeid et al., 2018b). 383

We confirmed RV infection of cells by RT-PCR and chose two levels of infection (MOI values 0.5 and 1) that resulted in infected cells but minimal cytopathic effect to allow the study of virus infection on NPs uptake. Virus infection by RV-A16 and RV-A01 either significantly (P < 0.05, P< 0.01, P < 0.001) increased or decreased NPs uptake compared to uninfected cells, depending on the experimental conditions. For HeLa cells, RV-A16 and RV-A01 infection elevated NPs uptake upon increasing the incubation time, but at longer timepoints (6h) a reduced uptake was noted with RV-A01 infection. The latter was likely due to decreased cell viability.

- 393 The picture with Beas-2B cells was more complex, with decreases in NP uptake observed at short incubation times following RV-A01 and RV-A16 infection. An increased incubation time (4h) was 394 associated with a marked decrease of NPs uptake for RV-A01 infected cells but an increase in 395 uptake with RV-A16 infected cells. It can be argued that the reduced HeLa cell viability after 396 infection or viral interference with the mechanism of NPs uptake due to different entry 397 mechanisms of major (RV-A16) and minor (RV-A01) group RVs are responsible for these 398 differences (Fuchs and Blaas, 2012). Furthermore, to observe these changes in NPs uptake, flow 399 400 cytometric analyses of the MFI was required since no changes in the percentage of cells taking up NPs were seen. However, it is clear that where there is an increased uptake of NPs, this is still 401 relatively minor when compared with our previous study (Abo-zeid et al., 2018b): when Huh7.5 402 403 cells were transfected with HCV (J6/JFH1 chimera), this resulted in a doubling of NPs uptake. J6/JFH1 is a recombinant HCV generated to maximize replication in cells in vitro. It was 404 developed from one HCV variant (JFH1) providing the non-structural components and another 405 406 strain (J6) providing the structural components to form the intra-genotypic HCV chimera (Lindenbach et al., 2005). It was found that J6/JFH1 chimera has both efficient RNA replication 407 and production of virus particle that could be transfected from culture media of infected Huh7.5 408 cells into naive Huh7.5 cells (Lindenbach et al., 2005). 409
- 410
- 411 The reasons behind the difference in NPs uptake between the cell lines could be both cell-related
- 412 and virus-related. Firstly, considering cell-related factors, in this study we used HeLa and Beas-
- 413 2B cells, selected for ease of infection *in vitro* and because they have been used extensively in
- 414 previous studies. During infection *in vivo*, RVs infect the airway epithelium. However, primary

415 <mark>e</mark>	endothelial cell	cultures	could no	ot be used	d in th	is study	y as the	e cells	are	difficult	to ol	otain	and
--------------------	------------------	----------	----------	------------	---------	----------	----------	---------	-----	-----------	-------	-------	-----

- 416 maintain *in vitro* for extended periods. Thus, we selected Beas-2B as a suitable alternative.
- 417
- 418 The HeLa and Beas-2B cells differ from each other and from the Huh7.5 cells used previously
- 419 (Abo-zeid et al., 2018b). The main route of NPs uptake into cells is the endocytic pathway
- 420 (Foroozandeh and Aziz, 2018). A previous study (Sayers et al., 2019) reported differences in the
- 421 endocytic pathways between cells types, including variations in the endolysosomal morphology,
- 422 localization, endocytic uptake, trafficking, recycling, endolysosomal pH, the ability of NPs to
- 423 escape the endosome prior to lysosomal sequestration or exocytosis. These differences have been
- 424 reported (Sayers et al., 2019) to affect the delivery of mRNA encapsulated into lipid NPs of 120
- 425 nm, and hence its expression efficiency. We expect that such differences in the endocytic pathway
- 426 among HeLa, Beas-2B and Huh7.5 cells could cause variations in NPs uptake.
- 427
- 428 Virus-related factors will also be important. In our previous study (Abo-zeid et al., 2018b), Huh7.5
- 429 cells were transfected with a genetically produced chimera virus (JFH1-J6 chimera), while in the
- 430 current study both HeLa cells and Beas-2B cells were infected with a whole active virus.
- 431 Additionally, viral structure, size and the entry mechanism into cells could have an effect. RVs are
- 432 non-enveloped viruses and have a positive-sense single stranded RNA genome that is protected by
- 433 an icosahedral protein capsid built of 60 copies each of the four viral capsid proteins VP1–VP4
- 434 (Stobart et al., 2017). In contrast, Hepatitis C virus (HCV) is an enveloped (E1-E2 glycoprotein
- 435 envelope) positive-sense single stranded RNA virus (Dustin et al., 2016). The particle size of RVs
- 436 is around 30 nm (Fuchs and Blaas, 2012) and HCV particle size is slightly larger, ranging from 40
- 437 to 80 nm (Calattini et al., 2015; Gastaminza et al., 2010).

438	\mathbf{RVs} we have used here have different mechanisms of entry into cells, as revealed in Figure 6. \mathbf{RVs}
439	A16 belongs to the major group of RVs and accesses the host cell by binding to ICAM-1 receptors.
440	while RV-A01 belongs to the minor group and binds to the low density lipoprotein receptor
441	(LDLR) at the surface of the host cell (Fuchs and Blaas, 2012). These events are followed by
442	clathrin mediated endocytosis, resulting in virion uncoating in the early endosome and late
443	endosome for RV-A16 and RV- A01 respectively. This is followed by release of the RV genome
444	into the cytosol for replication and production (Grove and Marsh, 2011). In contrast, HCV entry
445	requires binding to four receptors: CD81, SR-B1, Claudin-1, and Occludin (Pileri et al., 1998):
446	(Scarselli et al., 2002). Once bound to the cell, HCV is sorted by clathrin mediated endocytosis
447	and membrane fusion in the early endosome, followed by virus uncoating and release of genetic
448	material into the cytosol at the late endosome stage (Grove and Marsh, 2011). Virus infection
449	might therefore affect the rate of endocytic pathway uptake of NPs, resulting in either upregulation
450	or downregulation (or potentially have no effect). Consequently, effort should be devoted in the
451	future to study the effect of virus infection on the endocytic pathways to understand how (or if)
452	infection regulates the endocytic uptake of NPs.

453

Taken together, we hypothesis that differences in cell types, virus nature, virus size and virus entry mechanism will affect the physiology of the cell and hence have critical effects on the endocytic uptake of NPs. Therefore, future studies should be performed to elucidate the correlation between these factors and the uptake of NPs. Additionally, research modulating the physicochemical properties of NPs (material, morphology, size, zeta potential) and surface decoration (e.g. presence of ligands for active targeting of endocytic receptors of virus infected cells) to identify the key properties controlling their uptake into virus infected cells. Finally, the specific entry receptors 461 expressed at the surface of virus infected cells should be considered, since these could be
462 selectively targeted to assist with the future design of NPs for selective delivery of antiviral agents.
463

464 **4.** Conclusions:

465

This work involved development of four models of virus infected cells to probe the effect of virus 466 467 infection on NPs uptake. It was demonstrated that virus infection in some instances caused a 468 significant increase of NPs uptake compared to uninfected cells. For HeLa cells, RV-A16 and RV-A01 infection elevated NPs uptake upon increasing the incubation time, but at longer timepoints 469 470 (6h) a reduced uptake was noted with RV-A01 infection (owing perhaps to decreased cell 471 viability). With Beas-2B cells more complex trends are noted, with decreases in NPs uptake (cf. 472 uninfected cells) observed at short incubation times following RV-A01 and RV-A16 infection. However, an increased incubation time (4h) was associated with a marked decrease of NPs uptake 473 474 for RV-A01 infected cells while it led an increase in uptake with RV-A16 infected cells. Where increases in NPs uptake were found, they were very modest compared to results previously 475 reported for a hepatitis C/ Huh7.5 cell line model. We argue that the diverse endocytic pathways 476 among the different cell lines, together with changes in virus nature, size, and entry mechanism 477 are responsible for these differences. This work raises several questions regarding the application 478 of nanomedicine to improve antiviral therapy. To design potent medicines, it will be necessary to 479 480 understand how virus entry mechanism affects the endocytic pathway of cells, and whether this 481 can modify the uptake of NPs. Further, the subcellular signals of the endocytic pathway affected 482 following virus infection need to be elucidated, and there is an open question as to whether virus infection affects the exocytosis of NPs. Identification of receptors specifically expressed at the 483

484	surface of virus infected cells could permit the design of NPs to target infected cells, as could
485	greater understanding of how the physicochemical properties of NPs influence uptake.
486	
487	Declaration of interest
488	
489	The authors declare no conflicts of interest.
490	
491	Acknowledgment
492	
493	We would like to thank the British Council and Science and Technology Development Fund in
494	Egypt for awarding a Newton-Mosharafa Researcher Links Travel Grant to Dr. Yasmin Abo-zeid.
495	
496	References
497	Abo-zeid, Y., Garnett, M.C., 2020. Polymer nanoparticle as a delivery system for ribavirin: Do nanoparticle avoid
498	uptake by Red Blood Cells? J. Drug Deliv. Sci. Technol. 56, 101552.
499	https://doi.org/10.1016/j.jddst.2020.101552
500	Abo-Zeid, Y., Ismail, N.S., McLean, G.R., Hamdy, N.M., 2020. A Molecular Docking Study Repurposes FDA
501	Approved Iron Oxide Nanoparticles to Treat and Control COVID-19 Infection. Eur. J. Pharm. Sci. 153,
502	105465. https://doi.org/10.1016/j.ejps.2020.105465
503	Abo-zeid, Y., Mantovani, G., Irving, W.L., Garnett, M.C., 2018a. Synthesis of nucleoside-boronic esters
504	hydrophobic pro-drugs: A possible route to improve hydrophilic nucleoside drug loading into polymer
505	nanoparticles. J. Drug Deliv. Sci. Technol. 46, 354–364. https://doi.org/10.1016/j.jddst.2018.05.027
506	Abo-zeid, Y., Urbanowicz, R.A., Thomsonb, B.J., William L. Irvingb, A.W.T., Garnett, M.C., 2018b. Enhanced
507	nanoparticle uptake into virus infected cells: Could nanoparticles be useful in antiviral therapy? Int. J. Pharm.

- 508 547, 572–581. https://doi.org/10.1016/j.ijpharm.2018.06.027
- Adalja, A., Inglesby, T., 2019. Broad-Spectrum Antiviral Agents: A Crucial Pandemic Tool. Expert Rev. Anti.
 Infect. Ther. 17, 467–470. https://doi.org/10.1080/14787210.2019.1635009
- 511 Arruda, E., Crump, C.E., Rollins, B.S., Ohlin, A.N.N., Hayden, F.G., 1996. Comparative Susceptibilities of Human

512 Embryonic Fibroblasts and HeLa Cells for Isolation of Human Rhinoviruses. J. Clin. Microbiol. 34, 1277–
513 1279.

- Arruda, E., Pitkäranta, A., Witek, T.J., Doyle, C.A., Hayden, F.G., 1997. Frequency and natural history of rhinovirus
 infections in adults during autumn. J. Clin. Microbiol. 35, 2864–2868. https://doi.org/10.1128/jcm.35.11.28642868.1997
- 517 Bartlett, N.W., Slater, L., Glanville, N., Haas, J.J., Caramori, G., Casolari, P., Clarke, D.L., Message, S.D.,
- 518 Aniscenko, J., Kebadze, T., Zhu, J., Mallia, P., Mizgerd, J.P., Belvisi, M., Papi, A., Kotenko, S. V, Johnston,
- 519 S.L., Edwards, M.R., 2012. Defining critical roles for NF- k B p65 and type I interferon in innate immunity to
 520 rhinovirus. EMBO Mol. Med. 4, 1244–1260. https://doi.org/10.1002/emmm.201201650
- 521 Calattini, S., Fusil, F., Mancip, J., Dao Thi, V.L., Granier, C., Gadot, N., Scoazec, J.Y., Zeisel, M.B., Baumert, T.F.,
- 522 Lavillette, D., Dreux, M., Cosset, F.L., 2015. Functional and biochemical characterization of hepatitis C virus
- 523 (HCV) particles produced in a humanized liver mouse model. J. Biol. Chem. 290, 23173–23187.
- 524 https://doi.org/10.1074/jbc.M115.662999
- 525 Chawla, A., Wang, C., Patton, C., Murray, M., Punekar, Y., Ruiter, A. de C.S., 2018. A Review of Long-Term

526 Toxicity of Antiretroviral Treatment Regimens and Implications for an Aging Population. Infect. Dis. Ther. 7,

- 527 183–195. https://doi.org/10.1007/s40121-018-0201-6
- 528 Clercq, E. de, E., D.C., 2016. Approved antiviral drugs over the past 50 years. Clin. Microbiol. Rev. 29, 695–747.
 529 https://doi.org/10.1128/CMR.00102-15.Address
- 530 Dustin, L.B., Bartolini, B., Capobianchi, M.R., Pistello, M., 2016. Hepatitis C virus: life cycle in cells, infection and
- bost response, and analysis of molecular markers influencing the outcome of infection and response to
- 532 therapy. Clin. Microbiol. Infect. 22, 826–832. https://doi.org/10.1016/j.cmi.2016.08.025

- 533 Fiandra, L., Colombo, M., Mazzucchelli, S., Truffi, M., Santini, B., Allevi, R., Nebuloni, M., Capetti, A., Rizzardini,
- **534** G., Prosperi, D., Corsi, F., 2015. Nanoformulation of antiretroviral drugs enhances their penetration across the
- blood brain barrier in mice. Nanomedicine Nanotechnology, Biol. Med. 11, 1387–1397.
- 536 https://doi.org/10.1016/j.nano.2015.03.009
- 537 Foroozandeh, P., Aziz, A.A., 2018. Insight into Cellular Uptake and Intracellular Trafficking of Nanoparticles.
- 538 Nanoscale Res. Lett. 13, 339–341.
- Fuchs, R., Blaas, D., 2012. Productive entry pathways of human rhinoviruses. Adv. Virol. 2012.
 https://doi.org/10.1155/2012/826301
- 541 Fuchs, R., Blaas, D., 2009. The enigma of yellow fever in East Africa. Rev. Med. Virol. 19, 57–64.
 542 https://doi.org/10.1002/rmv
- 543 Garnett, M.C., Baldwin, R.W., 1986. Endocytosis of a monoclonal antibody recognising a cell surface glycoprotein
 544 antigen visualised using fluorescent conjugates. Eur. J. Cell Biol. 221, 214–221.
- 545 Gastaminza, P., Dryden, K.A., Boyd, B., Wood, M.R., Law, M., Yeager, M., Chisari, F. V., 2010. Ultrastructural
- and Biophysical Characterization of Hepatitis C Virus Particles Produced in Cell Culture. J. Virol. 84, 10999–
 11009. https://doi.org/10.1128/jvi.00526-10
- 548 Gaur, P.K., Mishra, S., Bajpai, M., Mishra, A., 2014. Enhanced oral bioavailability of Efavirenz by solid lipid
- 549 nanoparticles: In vitro drug release and pharmacokinetics studies. Biomed Res. Int. 2014.
- 550 https://doi.org/10.1155/2014/363404
- Greve, J.M., Davis, G., Meyer, A.M., Forte, C.P., Yost, S.C., Marlor, C.W., Kamarck, M.E., McClelland, A., 1989.
 The major human rhinovirus receptor is ICAM-1. Cell 56, 839–847. https://doi.org/10.1016/0092-
- **553** 8674(89)90688-0
- Grove, J., Marsh, M., 2011. The cell biology of receptor-mediated virus entry. J. Cell Biol. 195, 1071–1082.
 https://doi.org/10.1083/jcb.201108131
- Harvie, P., Désormeaux, A., Bergeron, M.C., Tremblay, M., Beauchamp, D., Poulin, L., Bergeron, M.G., 1996.
- 557 Comparative pharmacokinetics, distributions in tissue, and interactions with blood proteins of conventional

- and sterically stabilized liposomes containing 2',3'-dideoxyinosine. Antimicrob. Agents Chemother. 40, 225–
 229. https://doi.org/10.1128/aac.40.1.225
- 560 Henquell, C., Mirand, A., Deusebis, A.L., Regagnon, C., Archimbaud, C., Chambon, M., Bailly, J.L., Gourdon, F.,
- 561 Hermet, E., Dauphin, J.B., Labbé, A., Peigue-Lafeuille, H., 2012. Prospective genotyping of human
- rhinoviruses in children and adults during the winter of 2009-2010. J. Clin. Virol. 53, 280–284.
- 563 https://doi.org/10.1016/j.jcv.2011.10.009
- Hillaireau, H., Le Doan, T., Appel, M., Couvreur, P., 2006. Hybrid polymer nanocapsules enhance in vitro delivery
 of azidothymidine-triphosphate to macrophages. J. Control. Release 116, 346–352.
- 566 https://doi.org/10.1016/j.jconrel.2006.09.016
- 567 Hofer, F., Gruenberger, M., Kowalski, H., Machat, H., Huettinger, M., Kuechler, E., Blaas, D., 1994. Members of
- the low density lipoprotein receptor family mediate cell entry of a minor-group common cold virus. Proc.
- 569 Natl. Acad. Sci. U. S. A. 91, 1839–1842. https://doi.org/10.1073/pnas.91.5.1839
- 570 Irwin, K.K., Renzette, N., Kowalik, T.F., Jensen, J.D., 2016. Antiviral drug resistance as an adaptive process. Virus
 571 Evol. 2, 1–10. https://doi.org/10.1093/ve/vew014
- 572 Johnston, S.L., Pattemore, P.K., Sanderson, G., Smith, S., Lampe, F., Josephs, L., Symington, P., Toole, S. o.,
- 573 Myint, S.H., Tyrrell, D.A.J., Holgate, S.T., 1995. Community study of role of viral infections in exacerbations
- 574 of asthma in 9-11 year old children. Bmj 310, 1225. https://doi.org/10.1136/bmj.310.6989.1225
- 575 Kallinteri, P., Higgins, S., Hutcheon, G.A., St. Pourçain, C.B., Garnett, M.C., 2005. Novel functionalized

biodegradable polymers for nanoparticle drug delivery systems. Biomacromolecules 6, 1885–1894.

- 577 https://doi.org/10.1021/bm049200j
- Kiang, D., Yagi, S., Kantardjieff, K.A., Kim, E.J., Louie, J.K., Schnurr, D.P., 2007. Molecular characterization of a
 variant rhinovirus from an outbreak associated with uncommonly high mortality. J. Clin. Virol. 38, 227–237.
 https://doi.org/10.1016/j.jcv.2006.12.016
- Lembo, D., Donalisio, M., Civra, A., Argenziano, M., Cavalli, R., 2018. Nanomedicine formulations for the delivery
 of antiviral drugs: a promising solution for the treatment of viral infections. Expert Opin. Drug Deliv. 15, 93 –

- 583 114. https://doi.org/10.1080/17425247.2017.1360863
- 584 Lembo, D., Swaminathan, S., Donalisio, M., Civra, A., Pastero, L., Aquilano, D., Vavia, P., Trotta, F., Cavalli, R.,
- 585 2013. Encapsulation of Acyclovir in new carboxylated cyclodextrin-based nanosponges improves the agent's
 586 antiviral efficacy. Int. J. Pharm. 443, 262–272. https://doi.org/10.1016/j.ijpharm.2012.12.031
- 587 Lindenbach, B.D.M.J.E., Syder, A.J., Wo'lk, B., Timothy L. Tellinghuisen, Christopher C. Liu, Toshiaki
- 588 Maruyama, R.O.H., Burton, D.R., McKeating, J.A., Rice, C.M., 2005. Replication of hepatitis C virus in cell
- 589 culture. Science (80-.). 309, 623–626. https://doi.org/10.7124/bc.0007C9
- 590 Mäkelä, M.J., Puhakka, T., Ruuskanen, O., Leinonen, M., Saikku, P., Kimpimäki, M., Blomqvist, S., Hyypiä, T.,
- Arstila, P., 1998. Viruses and bacteria in the etiology of the common cold. J. Clin. Microbiol. 36, 539–542.
 https://doi.org/10.1128/jcm.36.2.539-542.1998
- 593 Meng, W., Parker, T.L., Kallinteri, P., Walker, D.A., Higgins, S., Hutcheon, G.A., Garnett, M.C., 2006. Uptake and
- 594 metabolism of novel biodegradable poly (glycerol-adipate) nanoparticles in DAOY monolayer. J. Control.
 595 Release 116, 314–321. https://doi.org/10.1016/j.jconrel.2006.09.014
- 596 Moyle, G., 2000. Clinical Manifestations and Management Nucleoside Analog-Related Mitochondrial Graeme
- 597 Moyle, MD, MBBS, Dip Genitourinury of Antiretroviral Toxicity Medicine. Clin. Ther. 22, 911–936.
- 598 Nicholson, K.G., Kent, J., Ireland, D.C., 1993. Respiratory viruses and exacerbations of asthma in adults. Br. Med.
 599 J. 307, 982–986. https://doi.org/10.1136/bmj.307.6910.982
- Nii-Trebi, N.I., 2017. Emerging and Neglected Infectious Diseases: Insights, Advances, and Challenges. Biomed
 Res. Int. 2017. https://doi.org/10.1155/2017/5245021
- Nowacek, A., 2010. NIH Public AccessNanoART, neuroAIDS and CNS drug delivery. Nanomedicine (Lond) 4,
 557–574. https://doi.org/10.2217/nnm.09.38.NanoART
- Ochekpe, N.A., Olorunfemi, P.O., Ngwuluka, N.C., 2009. Nanotechnology and drug delivery part 1: Background
 and applications. Trop. J. Pharm. Res. 8, 265–274. https://doi.org/10.4314/tjpr.v8i3.44546
- 606 Oventa, F.R.N., Tanzial, A.N.N.A.M.A.S., Olero, P.I.S., Orrocher, R.O.C., 2000. Hemolytic Anemia Induced by
- 607 Ribavirin Therapy in Patients With Chronic Hepatitis C Virus Infection : Role of Membrane Oxidative

608 Damage. Hepatology 31, 39–45. https://doi.org/10.1053/he.2000.5789

- 609 Papi, A., Bellettato, C.M., Braccioni, F., Romagnoli, M., Casolari, P., Caramori, G., Fabbri, L.M., Johnston, S.L.,
- 610 2006. Infections and airway inflammation in chronic obstructive pulmonary disease severe exacerbations. Am.
- **611** J. Respir. Crit. Care Med. 173, 1114–1121. https://doi.org/10.1164/rccm.200506-859OC
- 612 Peters, C.J., LeDuc, J.W., 1999. An Introduction to Ebola: The Virus and the Disease. J. Infect. Dis. 179, Six -xvi.
 613 https://doi.org/10.1086/514322
- 614 Pileri, P., Uematsu, Y., Campagnoli, S., Galli, G., Falugi, F., Petracca, R., Weiner, A.J., Houghton, M., Rosa, D.,
- Grandi, G., Abrignani, S., 1998. Binding of hepatitis C virus to CD81. Science (80-.). 282, 938–941.

616 https://doi.org/10.1126/science.282.5390.938

- 617 Pradhan, P., Pandey, A.K., Mishra, A., Gupta, P., Tripathi, P.K., Menon, M.B., Gomes, J., Vivekanandan, P.,
- Kundu, B., 2020. Uncanny similarity of unique inserts in the 2019-nCoV spike protein to HIV-1 gp120 and
 Gag. https://doi.org/10.1101/2020.01.30.927871.
- 620 Reddel, R.R., Ke, Y., Gerwin, B.I., McMenamin, M.G., Lechner, J.F., Su, R.T., Brash, D.E., Park, J.B., Rhim, J.S.,
- 621 Harris, C.C., 1988. Transformation of Human Bronchial Epithelial Cells by Infection with SV40 or
- 622 Adenovirus-12 SV40 Hybrid Virus, or Transfection via Strontium Phosphate Coprecipitation with a Plasmid
- 623 Containing SV40 Early Region Genes. Cancer Res. 48, 1904–1909.
- 624 Sayers, E.J., Peel, S.E., Schantz, A., England, R.M., Beano, M., Bates, S.M., Desai, A.S., Puri, S., Ashford, M.B.,
- 625 Jones, A.T., 2019. Endocytic Profiling of Cancer Cell Models Reveals Critical Factors Influencing LNP-
- 626 Mediated mRNA Delivery and Protein Expression. Mol. Ther. 27, 1–13.
- 627 https://doi.org/10.1016/j.ymthe.2019.07.018
- 628 Scarselli, E., Ansuini, H., Cerino, R., Roccasecca, R.M., Acali, S., Filocamo, G., Traboni, C., Nicosia, A., Cortese,
- 629 R., Vitelli, A., 2002. The human scavenger receptor class B type I is a novel candidate receptor for the
- 630 hepatitis C virus. EMBO J. 21, 5017–5025. https://doi.org/10.1093/emboj/cdf529
- 631 Schober, D., Kronenberger, P., Prchla, E., Blaas, D., Fuchs, R., 1998. Major and Minor Receptor Group Human
- 632 Rhinoviruses Penetrate from Endosomes by Different Mechanisms. J. Virol. 72, 1354–1364.

633

https://doi.org/10.1128/jvi.72.2.1354-1364.1998

- 634 Schuler, B.A., Schreiber, M.T., Li, L., Mokry, M., Kingdon, M.L., Raugi, D.N., Smith, C., Hameister, C.,
- 635 Racaniello, V.R., Hall, D.J., 2014. Major and Minor Group Rhinoviruses Elicit Differential Signaling and
- 636 Cytokine Responses as a Function of Receptor-Mediated Signal Transduction. PLoS One 9.
- 637 https://doi.org/10.1371/journal.pone.0093897
- 638 Shanks, G.D., Brundage, J.F., 2012. Pathogenic responses among young adults during the 1918 influenza pandemic.
- 639 Emerg. Infect. Dis. 18, 201–207. https://doi.org/10.3201/eid1802.102042
- Soota, K., Maliakkal, B., 2014. Ribavirin induced hemolysis : A novel mechanism of action against chronic hepatitis
 C virus infection. World J. Gastroenterol. 20, 16184–16190. https://doi.org/10.3748/wjg.v20.i43.16184
- 642 Stobart, C.C., Nosek, J.M., Moore, M.L., 2017. Rhinovirus biology, antigenic diversity, and advancements in the
- design of a human rhinovirus vaccine. Front. Microbiol. 8, 1–8. https://doi.org/10.3389/fmicb.2017.02412
- Szunerits, S., Barras, A., Khanal, M., Pagneux, Q., Boukherroub, R., 2015. Nanostructures for the inhibition of viral
 infections. Molecules 20, 14051–14081. https://doi.org/10.3390/molecules200814051
- 646 Winther, B., 2011. Rhinovirus infections in the upper airway. Proc. Am. Thorac. Soc. 8, 79–89.
- 647 https://doi.org/10.1513/pats.201006-039RN
- 648 Zhang, C., Zheng, W., Huang, X., Bell, E.W., Zhou, X., Zhang, Y., 2020. Protein structure and sequence re-analysis
 649 of 2019-nCoV genome does not indicate snakes as its intermediate host or the unique similarity between its
- spike protein insertions and HIV-1 2.
- 51 Zhang, T., Howell, B.A., Dumitrascu, A., Martin, S.J., Smith, P.B., 2014. Synthesis and characterization of glycerol-
- adipic acid hyperbranched polyesters. Polymer (Guildf). 55, 5065–5072.
- 653 https://doi.org/10.1016/j.polymer.2014.08.036

654

655